Performance and reliability improvement of La_2O_3/Al_2O_3 nanolaminates using ultraviolet ozone post treatment*

Ji-Bin Fan(樊继斌)[1,†], Hong-Xia Liu(刘红侠)[2], Bin Sun(孙斌)[1], Li Duan(段理)[1], and Xiao-Chen Yu(于晓晨)[1]

[1] School of Materials Science and Engineering, Chang'an University, Xi'an 710061, China

[2] School of Microelectronics, Key Laboratory of Wide Band-Gap Semiconductor Materials and Devices, Xidian University, Xi'an 710071, China

(Received 12 December 2016; revised manuscript received 29 January 2017; published online 30 March 2017)

La-based binary or ternary compounds have recently attracted a great deal of attention as a potential candidate to replace the currently used Hf-based dielectrics in future transistor and capacitor devices for sub-22 generation. However, the hygroscopic nature of La_2O_3 hampers its application as dielectrics in electron devices. To cope with this challenge, ultraviolet (UV) ozone post treatment is proposed to suppress the moisture absorption in the H_2O-based atomic layer deposition (ALD) La_2O_3/Al_2O_3 nanolaminates which is related to the residual hydroxyl/hydrogen groups after annealing. The x-ray photoelectron spectroscopy (XPS) and conductive atomic force microscopy (AFM) results indicate that the moisture absorption of the H_2O-based ALD La_2O_3/Al_2O_3 nanolaminates is efficiently suppressed after 600 °C annealing, and the electrical characteristics are greatly improved.

Keywords: La_2O_3/Al_2O_3 nanolaminates, atomic layer deposition, ultraviolet ozone post treatment, annealing

PACS: 77.55.D–, 82.80.Pv **DOI:** 10.1088/1674-1056/26/5/057702

1. Introduction

Recently, rare earth oxides, such as La-based binary or ternary compounds, are receiving a lot of attention for their potential use as the second generation high dielectric constant materials instead of the currently used Hf-based dielectrics in future transistor and capacitor devices.[1–3] These materials show interesting properties such as a high permittivity, large band gap, and high crystallization temperature.[4–6] To obtain the thin films, atomic layer deposition (ALD) is the preferred deposition technique because of its low deposition temperature, excellent thickness and composition control, and conformal growth.[7] For high-κ oxide ALD deposition, H_2O is a more commonly used oxidant than O_3 because O_3 is not stable and the expensive production equipment is always needed. However, due to the well-known hygroscopic nature of La_2O_3, exposure to ambient moisture can potentially deteriorate its dielectric properties such as roughness enhancement, large leakage current, and low dielectric constant.[8,9] Therefore, the dielectric properties should include the resistance to the moisture absorption. Mixing with a less hygroscopic oxide such as Al_2O_3 has been proved to stabilize the lanthanide oxide.[10] Furthermore, it combines the advantages of the high-κ of La_2O_3 and the chemical and thermal stability of Al_2O_3. However, the La_2O_3/Al_2O_3 nanolaminates may still suffer from the moisture absorption because H_2O tends to physisorb on the surface strongly and contributes to a high concentration of hydroxyl/hydrogen groups in the nanolaminates although the purge time is sufficient.

The ultraviolet (UV) ozone post treatment has been proposed as an effective method for suppressing the moisture absorption of La_2O_3 films in the air.[11] Furthermore, the UV ozone treatment can be used at low temperatures, preventing thick interface layer formation compared with oxygen ambient annealing at high temperature.[12] Since this topic can be crucial for the successful inclusion of high-κ dielectrics in electron devices, its potential application in the thin La_2O_3/Al_2O_3 nanolaminates is investigated in this paper. The La_2O_3/Al_2O_3 nanolaminates treated with or without an UV ozone post treatment are investigated by x-ray photoelectron spectroscopy (XPS), conductive atomic force microscopy (AFM), and electrical measurements. The results indicate that La_2O_3/Al_2O_3 nanolaminates treated with the UV ozone post treatment suppress the moisture absorption and improve the *C*–*V* characteristics.

2. Experiment

Prior to the deposition, 8–12 Ω·cm P-type Si(100) wafers were RCA cleaned and a 30 s dip in diluted HF solution was used to remove the native oxide, followed by a 60 s rinse in deionized water. Tris(isopropylcyclopentadienyl) lanthanum [$La(^iPrCp)_3$] was used as the lanthanum precursor and trimethylaluminum (TMA) was used as the aluminum precursor. The container of the lanthanum precursor was heated to 180 °C and the aluminum precursor was at room temperature, corresponding to the vapor pressure of 10 hPa to 15 hPa. When H_2O was used as the oxidant, the container was set at the room temperature, corresponding to a vapor pressure of 7 hPa. La_2O_3/Al_2O_3 nanolaminates were formed by the pe-

*Project supported by the National Natural Science Foundation of China (Grant Nos. 61604016 and 51501017) and the Fundamental Research Funds for the Central Universities, China (Grant No. 310831161003).

†Corresponding author. E-mail: jbfan@chd.edu.cn

© 2017 Chinese Physical Society and IOP Publishing Ltd

riodic stacking of bilayer structures to form thicker multilayers. Different thickness La_2O_3/Al_2O_3 nanolaminates were deposited on the Si substrates by ALD at 300 °C. Some samples were treated with UV ozone post treatment by an UV ozone ProCleaner plus system for 25 min at room temperature. After all the nanolaminates were annealed in nitrogen at 600 °C for 60 s, the XPS, AFM, and electrical measurements were carried out to investigate the characteristics of the La_2O_3/Al_2O_3 nanolaminates. The XPS measurements were carried out by using monochromatic Al $K\alpha$ x-ray ($h\nu = 1486.7$ eV). The AFM and CAFM measurements were carried out by a Bruker Dimension Edge system. The electrical measurements were carried out using a Keithley 590 C–V meter.

3. Results and discussion

Figure 1 shows the thickness and dielectric constant of the La_2O_3/Al_2O_3 nanolaminates. The thickness of all samples is measured by a Woollam M2000D spectroscopic ellipsometer. As shown in Fig. 1(a), the thickness of the La_2O_3/Al_2O_3 nanolaminates without UV ozone post treatment increases from 5.27 nm to 8.49 nm after annealing. This may be attributed to the absorption of moisture in the nanolaminates after annealing.[9] Furthermore, the thickness of the La_2O_3/Al_2O_3 nanolaminates with UV ozone post treatment decreases from 4.93 nm to 4.67 nm after annealing. This may be explained by the densification of the films after thermal annealing. The extracted dielectric constant ε is given in Fig. 1(b). The dielectric constant is determined as follows:

$$\mathrm{EOT}_{\mathrm{total}} = A\frac{\varepsilon_0\varepsilon_{\mathrm{SiO_2}}}{C_{\mathrm{OX}}}, \tag{1}$$

$$\mathrm{EOT}_{\mathrm{high}-k} = \mathrm{EOT}_{\mathrm{total}} - T_{\mathrm{SiO}_x}, \tag{2}$$

$$\varepsilon_{\mathrm{high}-k} = \frac{T_{\mathrm{high}-k}}{\mathrm{EOT}_{\mathrm{high}-k}}\varepsilon_{\mathrm{SiO_2}}, \tag{3}$$

where A is the area, C_{OX} is the accumulation capacitance of the La_2O_3/Al_2O_3 nanolaminates, and $\varepsilon_{\mathrm{high}-k}$ and $\varepsilon_{\mathrm{SiO_2}}$ are the permittivities of the La_2O_3/Al_2O_3 nanolaminate and SiO_2, respectively. The dielectric constant obtained for as-deposited La_2O_3/Al_2O_3 nanolaminates without UV ozone post treatment is 9.6 and it decreases to 6.7 after annealing. However, the dielectric constant for the La_2O_3/Al_2O_3 nanolaminates with UV ozone post treatment increases from 12.6 to 15.8 after annealing. The results indicate that the La_2O_3/Al_2O_3 nanolaminate with UV ozone post treatment has good thermal stability and relatively high dielectric constant.

Figure 2 shows the surface images of the La_2O_3/Al_2O_3 nanolaminates with and without UV ozone post treatment before and after annealing. As shown in Fig. 2, a smoother surface of La_2O_3/Al_2O_3 nanolaminate is observed and root mean square (RMS) roughness decreases after the UV ozone post treatment. Furthermore, the RMS roughness of the La_2O_3/Al_2O_3 nanolaminate without UV ozone post treatment increases sharply from 0.337 nm to 1.831 nm after annealing, whereas that of the La_2O_3/Al_2O_3 nanolaminate with UV ozone post treatment decreases from 0.267 nm to 0.060 nm. The RMS value of the La_2O_3/Al_2O_3 nanolaminate without UV ozone post treatment increases nearly 5.4 times after annealing possibly due to the formation of low density hexagonal $La(OH)_3$.[13] Due to the densification of the nanolaminate after annealing, the RMS value of the UV ozone post treated nanolaminate decreases nearly 4.5 times. The results suggest that, without UV ozone post treatment, the La_2O_3/Al_2O_3 nanolaminates deposited by ALD using H_2O as oxidant are still suffering from moisture absorption of La_2O_3 due to the residual hydroxyl/hydrogen groups, which is harmful to obtain good properties of La_2O_3/Al_2O_3 nanolaminate after annealing.

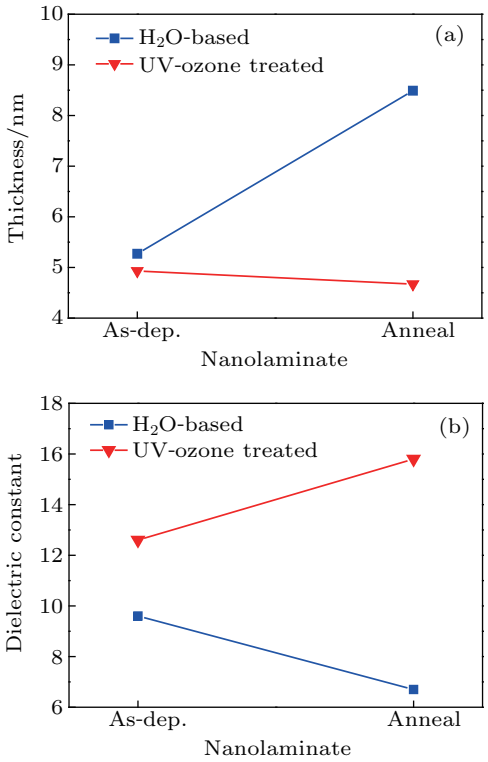


Fig. 1. (color online) (a) Thickness and (b) dielectric constant of the La_2O_3/Al_2O_3 nanolaminates before and after annealing.

In order to confirm that the moisture absorption occurs in the La_2O_3/Al_2O_3 nanolaminate without UV ozone post treatment after annealing, figure 3 shows the O_{1s} spectra of the La_2O_3/Al_2O_3 nanolaminates with and without UV ozone post treatment before and after annealing. For the H_2O-based La_2O_3/Al_2O_3 nanolaminate without UV ozone post treatment, the O_{1s} core level spectrum consists of four fitting peaks, which are located at binding energies of 529.18 eV, 530.28 eV, 531.03 eV, and 532.16 eV. These peaks are corresponding to the chemical bonds of La–O–La, La–O–Al, Al–O–Al, and La–O–H, respectively.[14] After annealing, the percentage composition of La–O–H chemical bond increases from 4.73 at.% to 15.26 at.%. It can be concluded that the forma-

tion of $La(OH)_x$ occurs obviously due to the residue of hydroxyl/hydrogen groups in the layers after annealing. For the H_2O-based La_2O_3/Al_2O_3 nanolaminate with UV ozone post treatment, the O_{1s} core level spectrum consists of four fitting peaks, which are located at the binding energies of 528.99 eV, 530.01 eV, 531.21 eV, and 532.44 eV. These peaks correspond to the chemical bonds of La–O–La, La–O–Al, Al–O–Al, and La–O–H, respectively.[14] After annealing, the percentage of La–O–H chemical bond increases slightly from 3.89 at.% to 3.97 at.%. Since the UV ozone post treatment is considered to have an effect in terms of oxygen vacancy healing or enhancing the kinetics of oxidation,[12] it can suppress the vacancies reacted with water to form OH^- groups. It is reasonable to attribute the origin of the moisture absorption suppression to the UV ozone post treatment which heals oxygen vacancies in the nanolaminates. Furthermore, despite the increase of the La–O–Al peak intensity leading to the peak intensity of La–O–La and Al–O–Al decreased obviously after annealing for the La_2O_3/Al_2O_3 nanolaminates with and without UV ozone post treatment, the significant decreasing of La–O–La peak intensity for the La_2O_3/Al_2O_3 nanolaminate without UV ozone post treatment is also attributed to the increase of the La–O–H peak intensity.

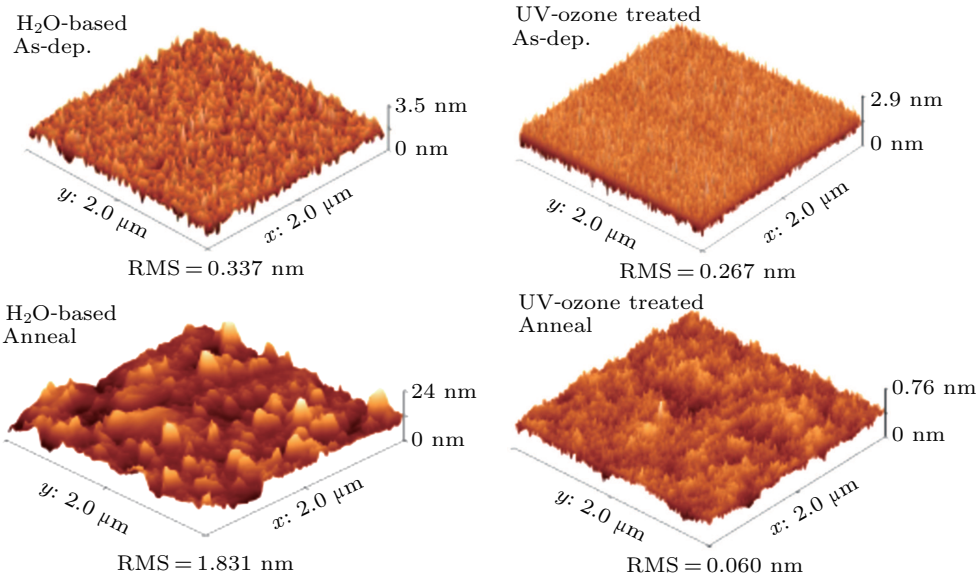


Fig. 2. (color online) AFM surface images of La_2O_3/Al_2O_3 nanolaminates without and with UV ozone post treatment before and after annealing.

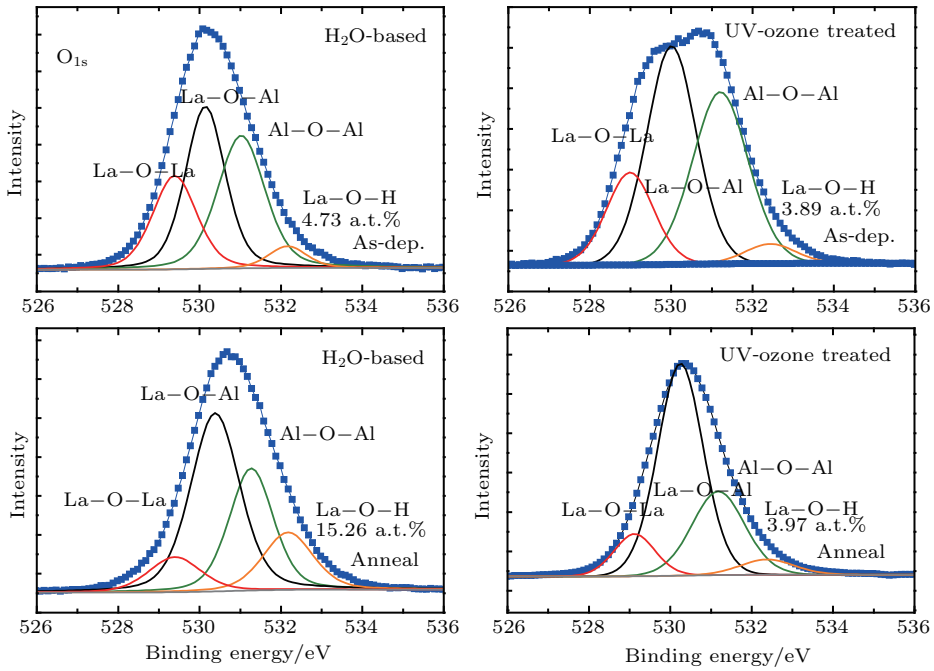


Fig. 3. (color online) O_{1s} spectra of La_2O_3/Al_2O_3 nanolaminates without and with UV ozone post treatment before and after annealing.

Figure 4 shows the current images of the La_2O_3/Al_2O_3 nanolaminates with and without UV ozone post treatment before and after annealing. The current images are measured by conductive AFM when applying a sample bias of 3 V. The current images provide information on the spatial conductivity distribution of the La_2O_3/Al_2O_3 nanolaminates.

As shown in Figs. 4(a) and 4(b), the density of leakage spots in the La_2O_3/Al_2O_3 nanolaminates without UV ozone post treatment increases obviously after annealing, and these spots exhibit large leakage currents. They are not only attributed to surface roughness, but also possibly caused by local fluctuations in composition and/or structures, and/or by defects in the nanolaminates. After UV ozone post treatment, as shown in Figs. 4(c) and 4(d), the density of leakage spots in the La_2O_3/Al_2O_3 nanolaminates decreases and the leakage current is smaller after annealing. The results indicate that, without UV ozone post treatment, the conductive paths for the La_2O_3/Al_2O_3 nanolaminates increase significantly after annealing due to the absorption of moisture generated kinds of defects and local structural changes, which correlate to the leakage spots increasing. The UV ozone post treatment suppresses the moisture absorption in the La_2O_3/Al_2O_3 nanolaminates and a less conductive feature is observed.

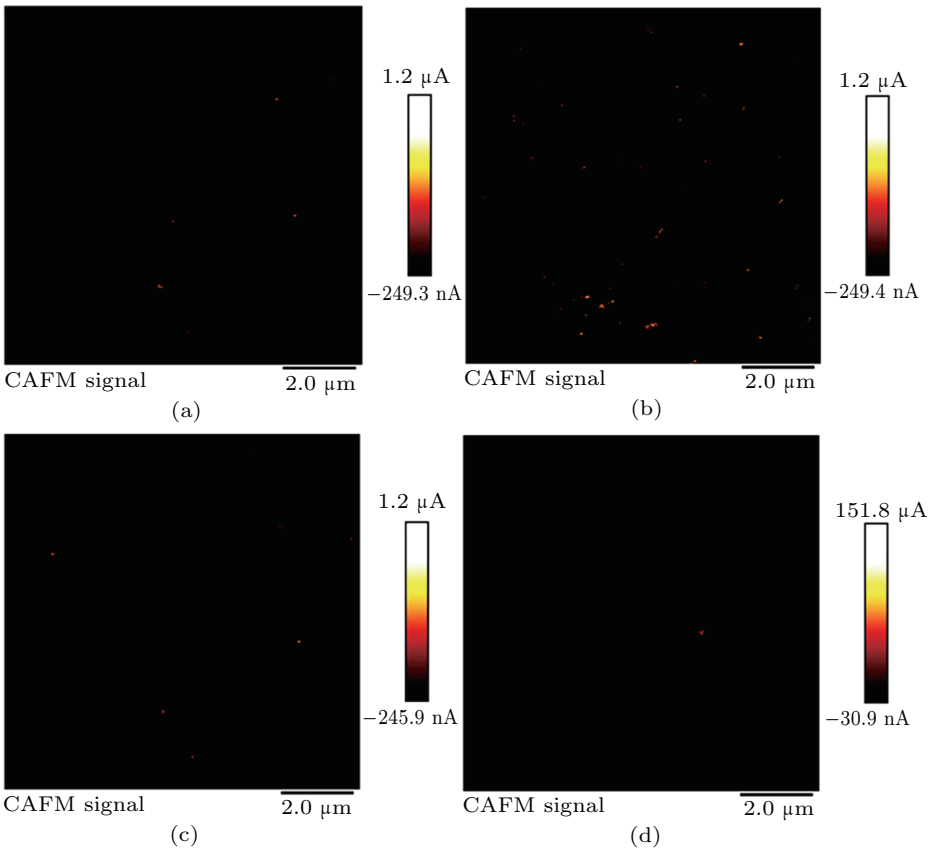


Fig. 4. (color online) CAFM images of H_2O-based La_2O_3/Al_2O_3 nanolaminates: (a) as-deposited, (b) annealed, (c) as-deposited nanolaminate with UV ozone treatment, and (d) annealed nanolaminate with UV ozone treatment.

In order to evaluate the moisture absorption effect on the properties of the La_2O_3/Al_2O_3 nanolaminates before and after annealing, the valence band offset is determined by using the method proposed by Kraut[15]

$$\begin{aligned}\Delta E_{\mathrm{VBO}} = {} & (E_{\mathrm{CL}}^{\mathrm{Si2p}} - E_{\mathrm{V}})_{\mathrm{bulk,Si}} \\ & - (E_{\mathrm{CL}}^{\mathrm{Al2p}} - E_{\mathrm{V}})_{\mathrm{thick\ nanolaminate}} \\ & - (E_{\mathrm{CL}}^{\mathrm{Si2p}} - E_{\mathrm{CL}}^{\mathrm{Al2p}})_{\mathrm{thin\ nanolaminate/Si}}, \end{aligned} \quad (4)$$

where $E_{\mathrm{CL}}^{\mathrm{Si2p}}$ and $E_{\mathrm{CL}}^{\mathrm{Al2p}}$ are the binding energies of the Si_{2p} and Al_{2p} shallow core levels, respectively, and E_{V} is the binding energy corresponding to the valence band maximum (VBM). The position of the VBM is determined by using the linear method. The energy difference between these core levels and the corresponding valence band maxima E_{V} in bulk Si and thick La_2O_3/Al_2O_3 nanolaminate are determined. By measuring the energy difference between two shallow core levels in thin nanolaminates on Si, the VBO of the La_2O_3/Al_2O_3 nanolaminates can be calculated. According to the early work, the energy difference between the Si_{2p} and VBM is 98.90 eV for bulk clean Si sample as measured by XPS.[16]

Figure 5 shows the XPS core-level spectra of Si_{2p} and Al_{2p} for the La_2O_3/Al_2O_3 nanolaminates with and without UV ozone post treatment before and after annealing. The core level energies are obtained by curve fitting to ensure high accuracy binding energy of the peak and the spectra are referenced to the C_{1s} peak at 284.8 eV. As shown in Figs. 5(a)–

5(d), the energy difference between the core levels are calculated. Using these energy differences and Eq. (4), we obtain VBO of 3.71 eV and 4.16 eV for the as-deposited and the annealed La_2O_3/Al_2O_3 nanolaminates without UV ozone post treatment, respectively. For the La_2O_3/Al_2O_3 nanolaminates with UV ozone post treatment, the VBO changes from 2.74 eV to 2.85 eV after annealing. Compared with the negligible VBO variation for the La_2O_3/Al_2O_3 nanolaminates with UV ozone post treatment after annealing, a larger VBO variation for the La_2O_3/Al_2O_3 nanolaminates without UV ozone post treatment may be explained by the large amount of oxygen vacancies that are generated accompanied with the absorption of moisture.

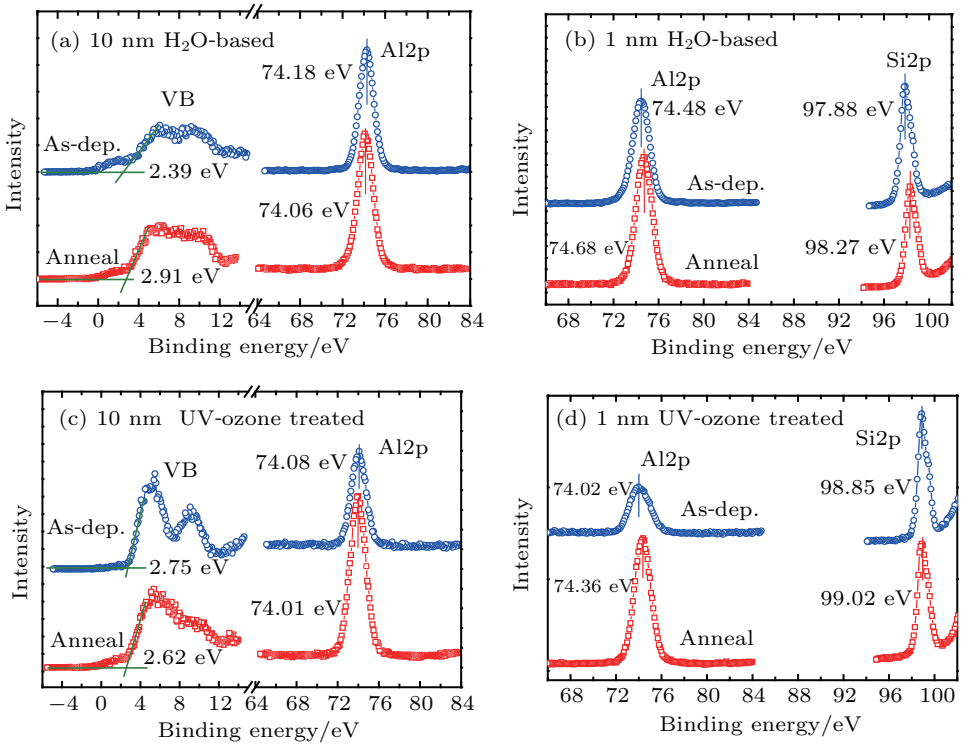


Fig. 5. (color online) The XPS core-level spectra of Si_{2p} and Al_{2p} for (a), (c) 10 nm and (b), (d) 1 nm La_2O_3/Al_2O_3 nanolaminates before annealing (as-dep.) and after annealing (annealed).

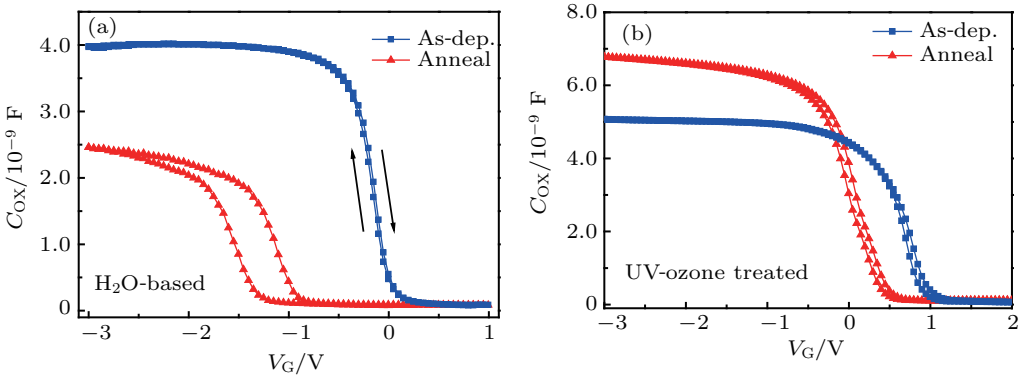


Fig. 6. (color online) The *C*–*V* characteristics of (a) H_2O-based nanolaminates and (b) H_2O-based La_2O_3/Al_2O_3 nanolaminates with UV ozone post treatment before and after annealing ($f = 100$ kHz).

The band offset change after annealing should result in a shift in V_{FB}.[17,18] Figure 6 shows the *C*–*V* characteristics of 5 nm La_2O_3/Al_2O_3 nanolaminates with and without UV ozone post treatment before and after annealing ($f = 100$ kHz). The gate voltage (V_G) is swept from accumulation to inversion and then swept back. For the H_2O-based La_2O_3/Al_2O_3 nanolaminates, as shown in Fig. 6(a), the hysteresis in the *C*–*V* curves increases significantly and the capacitance of the La_2O_3/Al_2O_3 nanolaminates decreases after annealing. It can be explained by the moisture absorption of La_2O_3 deteriorating the properties of the nanolaminates and generating a large amount of defects. Furthermore, the *C*–*V* curves shift from the positive to the negative direction after annealing, which shows that the positive charge increases after annealing; this

is associated with the oxygen vacancies generation. For the La_2O_3/Al_2O_3 nanolaminates with UV ozone post treatment, as shown in Fig. 6(b), due to the densification of La_2O_3/Al_2O_3 nanolaminates and decrease of the impurities concentration, the accumulation capacitance increases after annealing. The results indicate that the UV ozone post treatment successfully suppresses the moisture absorption and thus better electrical characteristics are observed after annealing, which is consistent with the AFM and XPS results.

4. Conclusion

The electrical properties of H_2O-based ALD La_2O_3/Al_2O_3 nanolaminates on the Si substrate can be substantially improved by UV ozone post treatment after annealing. Moisture absorption occurs obviously for the non UV ozone post treatment samples after annealing, whereas it is suppressed in the UV ozone post treatment samples. The XPS results indicate that the UV ozone post treatment has the effect of oxygen vacancy healing and suppressing the vacancies reacted with water to form OH^- groups. As a result, a small thickness variation, a smooth roughness surface, and negligible VBO variation are observed for the UV ozone post treated samples compared with the non UV ozone post treated samples after annealing. The current images measured by CAFM and the *C*–*V* measurement results indicate that after UV ozone post treatment, the La_2O_3/Al_2O_3 nanolaminates present a good *C*–*V* characteristic, high permittivity, and less conductive feature.

References

[1] Gupta S, Gong X, Zhang R, Yeo Y C, Takagi S and Saraswat K C 2014 *MRS Bull.* **39** 678
[2] McDaniel M D, Ngo T Q, Hu S, Posadas A, Demkov A A and Ekerdt J G 2015 *Appl. Phys. Rev.* **2** 041301
[3] Fei C X, Liu H X, Wang X, Zhao D D, Wang S L and Chen S P 2016 *Chin. Phys. B* **25** 058106
[4] Kim J, Kim H C, Wallace R M and Park T J 2012 *ECS Trans.* **45** 95
[5] Choi M, Janotti A and Walle C G V D 2013 *Phys. Rev. B* **88** 214117
[6] Lim S G, Kriventsov S, Jackson T N, Haeni J H, Schlom D G, Balbashov A M, Uecker R, Reiche P, Freeouf J L and Lucovsky G 2002 *J. Appl. Phys.* **91** 4500
[7] Fan J B, Liu H X, Ma F, Zhuo Q Q and Hao Y 2013 *Chin. Phys. B* **22** 027702
[8] Li X, Mao X, Feng M, Qi S, Jiang B and Zhang L 2016 *J Eur. Ceram. Soc.* **36** 2549
[9] Zhao Y, Kita K, Kyuno K and Toriumi A 2007 *Jpn. J. Appl. Phys.* **46** 4189
[10] Wang X, Liu H X, Fei C X, Yin S Y and Fan X J 2015 *Nanoscale Res. Let.* **10** 1
[11] Zhao Y, Kita K, Kyuno K and Toriumi A 2007 *Jpn. J. Appl. Phys.* **46** 1
[12] Song W J, So S K, Wang D, Qiu Y and Cao L 2001 *Appl. Surf. Sci.* **177** 158
[13] Nieminen M, Putkonen M and Niinistö L 2001 *Appl. Surf. Sci.* **174** 155
[14] Kim H, Woo S, Lee J, Kim H, Kim Y, Lee H and Jeon H 2010 *J Electrochem. Soc.* **157** 479
[15] Kraut E A, Grant R W, Waldrop J R and Kowalczyk S P 1983 *Phys. Rev. B* **28** 1965
[16] Fan J B, Liu H X, Gao B, Ma F, Zhuo Q Q and Hao Y 2012 *Chin. Phys. B* **21** 087702
[17] Fortunato E, Barquinha P and Martins R. 2012 *Adv. Mater.* **24** 2945
[18] Chang I Y, You S, Juan P, Wang M and Lee J Y 2009 *IEEE Electron Device Lett.* **30** 161